Multi-Service Battery Energy Storage System Optimization and Control

Sarmad Hanif, M. J. E. Alam, Kini Roshan, Bilal A. Bhatti, Juan C. Bedoya[a]

[a]*Pacific Northwest National Laboratory, 902 Battelle Boulevard, Richland, 99352, WA, USA*

Abstract

Battery energy storage systems (BESS) have become a fundamental part of modern power systems due to their ability to provide multiple grid services. As renewable penetration increases, BESS procurement is also expected to increase and is envisioned to play a systematic and strategic role in power systems planning and operation. Therefore, in this paper we present a multiple grid service procurement and operation approach for BESS, including energy arbitrage, reserve/regulation services, power factor correction, and demand management. The proposed framework considers an optimal multi-temporal dimension and is designed to be operable for both planning and real-time operation. Moreover, the nonlinearity inherent to BESS services and the uncertainty associated with market forecast variables are addressed using techniques such as polyhedral norms and robust optimization approaches. The developed model is tested using a utility-scaled BESS, and the results show the effectiveness of the systematic BESS multi-service planning and operation approach.

Keywords: Battery energy storage system (BESS), Convex Optimization, Multi-Service, Uncertainty, Real-Time Control.

Nomenclature

⋆This work is sponsored by PNNL, operated by Battelle for the U.S. Department of Energy under Contract DE-AC05-76RL01830.

$\mathbb{T}_d, \mathbb{T}_r, \mathbb{T}_h$	Demand charge, regulation power, and hourly time set
t_d, t_r, t_h	Time step in the demand charge, regulation, and hourly time set
p_d, p_c, p_b	Battery discharge, charge, and net injection
p_g, p_l	Power import from the grid and local demand
$p_+(t), p_-(t)$	Regulation up and down participation
ρ, ρ_+	Power factor and its limits
λ_r, λ_e, λ_{pk}	Reserve, energy, and peak price
Λ^r, Λ^e, $\mathcal{P}_L$	Reserve price, energy price, and local demand uncertainty set
$\Gamma^{R/A/D}$	Reserves/Arbitrage/Demand charge problem's uncertainty budgets
$(\zeta_{R/A/D}, \beta_{R/A/D})$	Reserves/Arbitrage/Demand charge problems' dual variable from robustification
$p_g(t), q_g(t), s_g(t)$	Total active, reactive, and apparent power seen at the grid at each time step t
$p_b(t), q_b(t), s_b(t)$	Total BESS active, reactive, and apparent power at each time step t
$p_l(t), q_l(t), s_l(t)$	Total active, reactive, and apparent load at each time step t
s_{max}	Maximum apparent power rating for the inverter
η_c, η_d	BESS charging and discharging efficiency in per-unit
$x(t)$	BESS state of charge at time t
Δt	Time step in an hour
R_A	Revenue from energy arbitrage in \$
R_R	Revenue from reserve/regulation provision in \$
C_D	Cost of demand charge reduction in \$
C_{PF}	Cost of power factor correction in \$
λ_{mis}	Penalty factor for reserve/regulation provision
p_{max}, x_{max}	BESS maximum power and state of charge limit
p_{pk}	Auxiliary variable in demand charge formulation

$\tilde{(\cdot)}$ and $\hat{(\cdot)}$ represents the predicted and actual value of quantity $(\cdot)$, respectively and $|a + i \cdot b|$ represents the absolute value of the complex quantity as $\sqrt{a^2 + b^2}$, with the real and imaginary value denoted by a and b, respectively.

1. Introduction

Due to the growing penetration of renewable resources and proactive prosumers, higher grid flexibility and smart operation is required to maintain reliability and safe operations. Under such requirements, the role of the battery energy storage system (BESS) is becoming more and more important [1]. According to [2], the penetration of BESS in power grids across the world is expected to reach 8.6 GW and 21.6 GWh by 2022. As prime importance for power grids is their security, the earlier applications concerning BESS have been focused primarily on addressing grid reliability. The authors in [3] studied the effects of sizing BESS to support grid reliability. The method outlined an approach to consider BESS within the framework of mitigative actions from the demand response and dynamic thermal rating for higher grid reliability. In [4], a genetic algorithm and fuzzy logic-based method are proposed to optimize the BESS capacity and line thermal rating to increase network reliability. Similarly in [5], the authors evaluated the use of BESS to mitigate the intermittent nature of wind power for higher reliability. However, the main reasons for the popularity of BESS stems from the fact that it can not only support the power grid reliability, but can also provide multiple grid services and hence financial benefits to its owners [6]. Ultimately, which leads to the reduction in BESS acquisition costs [7]. Indeed, the most economically beneficial operation of BESS is usually found when it is operated to provide multiple services [8, 9]. Hence, in this paper, we study BESS which procures multiple services.

Before we present the state-of-the-art research on multiple services by BESS, we would like to point out a few field/real-life capability demonstrations of BESS to support multiple services. Early efforts to control the real and reactive power of the 10 kVA/30 kWh BESS to provide peak load support in a laboratory setup were reported in [10] showed that utility-scale BESS 1 MW/3.2 MWh may even be operated using a multi-layered control architecture framework with possibilities of local (volt/var) and system-wide (transmission grid deferral) services. In [11], multiple applications were investigated (frequency regulation and reactive power compensation) for the BESS project of 1.2 MVA/600 kWh energy power/capacity with 900 kVar reactive power capability from Helen Electricity Network Ltd. (Helsinki). ComEd, a utility, conducted a first-of-its-kind community storage pilot to demonstrate power outage mitigation and 750 kW solar power integration, with the help of a 500 kW/2MWh BESS [12]. Adaptive PV power smoothing is demonstrated in a field test using 130kWh/125kW BESS while avoiding excessive battery use so that it can provide other grid services[13].

The academic research advocating multi-service procurement from BESS has gained a lot of attention from the researchers around the world. BESS to support multi-services have also been proposed using real-time controllers [14, 15] or considering local constraints to be included in their look-ahead planning methods in [16, 17]. In [14] autonomous real-time controllers were proposed to react to grid disturbances, whereas in [15], the authors proposed simultaneous provision of active and reactive power from BESS. These works have not considered accounting for the planning phase of BESS which generates the economically feasible setpoints. Authors in [16, 17] proposed BESS planning methods to include grid constraints. However, the methods do not cover real-time control of those constraints, which is important as uncertainties may exist in the actual operation. From a technical and economical perspective, as one may suspect, the most cognizant methodology utilizes both the predicted (look-ahead) as well as the real-time conditions for smooth BESS operation.

A two-phase framework for controlling and scheduling energy storage is presented in [18] to provide multiple services to the grid. In the first phase, a rolling horizon-based period-ahead planning is implemented to maximize the storage capacity and continue the operation of the storage system. In the second stage, the storage power is computed in real-time for each service and superimposed on the period-ahead planning. However, non-convexities associated with the grid constraints have not been considered, which may challenge the computationally inexpensive method proposed in [18]. Also, the method does not explicitly consider uncertainties in the planning phase which may create the energy budget calculation proposed in [18] to be way-off in the real-time control phase. A co-optimization methodology with energy storage to consider grid constraints (power factor correction) is developed in [19] using a McCormick relaxation optimization. However, in [19], the authors do not consider the uncertainties associated with the planning stage explicitly, and instead proposed a receding horizon control which may get computationally inefficient to be solved repeatedly, as a higher number of services are included in the framework.

To safeguard the planning stage against uncertainties, optimization methods such as (1) stochastic optimization and (2) robust optimization may be deployed to explicitly address uncertainties. Using stochastic optimization, [20] analyzed the integration of BESS into the wholesale market; [21] and [22] demonstrated sizing of BESS for demand management and outage management in distribution grids, respectively and; [23] presented the utilization of BESS in the expansion planning of a transmission grid. The above-mentioned methods on stochastic optimization did not provide any treatment of the generated setpoints from the optimization in the real-time control. Moreover, these methods do not consider multiple services in their optimization. Hence, these works are not able to comment on the proposed methods' scalability and generalizability. A behind-the-meter BESS with a stochastic scheduling algorithm to jointly optimize frequency regulation and peak shaving is presented in [24]. The method in [25], though proposed for multiple services and catered for the real-time control, did not consider the non-convex nature of the grid constraints, which is challenging given the number of scenarios to be utilized with the stochastic variables increase exponentially with an increase in the number of constraints. Because the core of stochastic optimization lies in estimating the distribution of the uncertain variable, such method poses some challenges for multi-service procurement of BESS, such as (1) the distribution function to characterize uncertainty may create complications in recasting the stochastic program to be solved efficiently, (2) there may exist a large number of scenarios to cover the uncertainty range, making the optimization problem very large and/or intractable, and 3) for new BESS services there may not be enough data to quantify the prediction of the associated uncertain variables. Under such cases, robust optimization provides a computationally friendly mechanism to include uncertainty in the optimization problem. The authors in [26] included robust demand uncertainty sets in calculating demand charge reduction from BESS. The use of price uncertainty in the energy arbitrage of BESS is shown in [27]. The works in [28] solved for a robust investment decision for BESS when performing peak shaving. The works in [26, 27, 29] though utilized a computationally friendly robust optimization in the planning of BESS for grid services, did not consider the extension of their respective methods to multiple services as well as to the real-time control capability. Multiple services planning and control framework has been proposed in [30]. In [30], the method to optimize an integrated PV-BESS set to provide voltage and frequency control under uncertain solar irradiation, load prediction, and frequency regulation signal. As robust optimization solves for the worst-case scenario, the associated conservatism may be dealt with using the budget of uncertainty concept [31], making the solution less conservative while improving the solution time. However, the method in [30] parameterized the planning and control problem in terms of physical signals (e.g., load profile, local generation, and frequency measurements etc.), and not in terms of economic conditions (e.g., wholesale energy price, reserve price, power factor penalty, and demand charges etc.). As motivated earlier, evaluating monetary benefits are essential for the widespread integration of BESS in the power grid as they may hinder performance economic feasibility of potential BESS installations.

The pitfalls of the state-of-the-art literature on BESS multi-services procurement are summarized in Table 1, where it can be concluded that an extensive, scalable and a generic multi-services framework is missing. This paper presents such a framework which has the following novel contributions:

1. We provide a procedure to explicitly address wide-range of services pertaining to behind-the-meter, system-wide, and reactive power applications, namely: (1) energy arbitrage, (2) demand charge reduction, (3) reserve/regulation provision, and (4) power factor correction. Moreover, we provide a real-time correction procedure that utilizes real-time operating conditions and explicitly includes their impact to adjust the set points to accommodate each service. Table 1 shows that none of the state-of-the-art literature on BESS multi-services frameworks have explicitly addressed these wide-range of services in a common planning and control framework.
2. We show that the presented set of services can, in fact, be generalized to many more services by presenting a simplifying framework for the look-ahead planning stage that is based on the highest-time-resolution service (e.g., day-ahead energy arbitrage with hourly resolution) and then performing real-time correction based on the lowest-time-resolution (e.g., frequency regulation with 2-4 seconds resolution) service.
3. In the planning stage problem, despite diverse services provision, we provide a linear programming based framework such that the solution can be efficiently obtained in a timely manner using a common off-the-shelf solver. The issues addressed in this paper that hinder achieving a linear program in the presence of selected services are: (1) multiple temporal dimension, (2) non-convexity constraints, (3) min-max structure, and (4) uncertainty related to external variables.
4. The planning stage is augmented by real-time control, where a sensitivity-based control algorithm is utilized for timely decision of charge/discharge for the BESS. Similar to the planning stage, the real-time control laws

Table 1: Existing multi-service frameworks in the literature; services considered in the literature are named as: Demand Charge/Peak Load/Load Management (LO), Energy Arbitrage (EA), Reserve/Regulation/Primary Frequency (AS), Power Factor Correction/Voltage Support/Grid Constraints (GR); W0-U stands for without uncertainty and W-U stands for with uncertainty

Refs.	Services	Planning		Control	Remarks
		W0-U	W-U		
[14, 15]	AS + GR	X	X	✓	Novel real-time controllers without demonstrating planning of set-points
[19]	EA + GR	✓	X	X	No explicit uncertainty representation in the planning stage
[18]	EA + AS + LO	✓	X	✓	Non-convexities of grid constraints and explicit uncertainties not addressed
[24]	AS + LO	X	✓	✓	Non-convexities of grid constraints not addressed
[30]	AS + GR	X	✓	✓	Economic variables and associated uncertain parameters not addressed in robust optimization

are shown to be extensible to multi-services and generalizable for any service to be procured by BESS. This is done by assigning the associated parameters and variables of each service to be included explicitly in its control law.

The rest of this paper is organized as follows: Section II presents system setup and considered services for the novel approach. Sections III and IV describe the proposed day-ahead and real-time methodologies, respectively. Section V details the simulation results of the proposed strategy.

2. System Setup & Considered Services

2.1. Organizational and Functional Framework of BESS

In power grids, BESSs can be owned by residential users [32], a utility company [33], and a third-party company [34]. The BESS ownership model is dictated by the relevant services to be offered by the BESS. For example, participating in the energy wholesale market for exploring arbitrage opportunities requires a minimum capacity to be purchased/sold, which is usually much higher than the residential BESS (a few kWs) [35]. Note that, aggregation of multiple small-scale residential consumers may be done to meet such conditions, however, such models are subjected to further scrutiny by the regulators and require careful administration. With the advent of the FERC Order 2222 [36], these aggregation services are destined to get more advanced and their adoption in the ownership models may become widespread. Hence, in the current grid realm, utility-scale BESSs (100s of kWs to MWs power capacity) are explored to provide grid services [37]. Hence in this paper, to explore multiple services and bypass addressing the barriers existing in the regulatory framework, we adopt a utility-scale BESS ownership model. The operational assumptions of the chosen ownership models are:

1. The BESS is assumed to be either operated by the utility or a company for the utility such that it provides certain services based on its contractual agreement.
2. It is assumed that the relevant data for optimizing services for the grid, the appropriate battery management system to monitor BESS SoC, and proper regulation of BESS strings to achieve the requested charge/discharge setpoints is overseen by the BESS owner.
3. The services to be procured by the BESS are supported by the current market rules.

4. If multiple BESSs exist in the system, the BESS owner aggregates them to a common point, and hence the proposed method of this paper considers them to be operable as a single BESS.
5. The utility has already performed hosting capacity analysis for the installed BESS in the grid, such that the maximum charge/discharge of the BESS does not cause any major voltage violation across the network, as well as does not cause any alarming levels of contribution in the fault current.

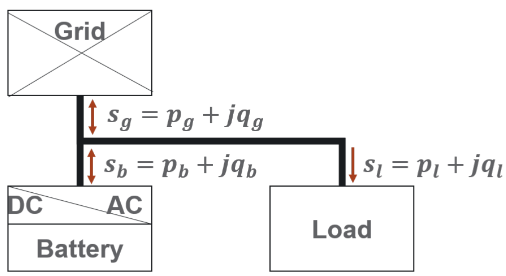

Figure 1: System setup with physical connection shown with black lines and power flow directions with blue arrows

2.2. Operational Models

Figure 1 shows the power flow configuration of the assumed setup of this paper. With this configuration, the total active p_g and reactive q_g power seen at the grid at each time step t is given as

$$p_g(t) = p_b(t) + p_l(t), \tag{1a}$$
$$q_g(t) = q_b(t) + q_l(t). \tag{1b}$$

The reactive $q_l(t)$ and active $p_l(t)$ power loads are considered to be fixed (measurements/historic forecast), whereas the active $p_b(t)$ and reactive power $q_b(t)$ are assumed to be controllable and can be related as

$$s_b = |p_b + iq_b| \leq s_{max} \tag{2}$$

where s_b is the apparent power injection/withdrawal by ESS and is constrained because of the inverter rating s_{max}. The battery (active) power p_b is the combination of its charging/discharging power p_c/p_d and efficiency factor η_c/η_d, such that:

$$p_b(t) = \frac{p_d(t)}{\eta_d} - \eta_c p_c(t). \tag{3}$$

The ESS energy level as a state-of-charge x can be obtained as:

$$x(t+1) = x(t) + p_b(t)\Delta t, \tag{4}$$

where Δt is the time step in an hour, with p_b given in kW and SoC in kWh. To conclude the apparent power, s_g seen at the grid can be shown as:

$$s_g = |p_g + iq_g| \tag{5}$$

2.3. Services Provision

To enhance the value obtained from the ESS, it is assumed that it can provide multiple services, as described below.

Energy Arbitrage. ESS attempts to improve its monetary benefit by charging (buying) when prices are low and discharging (selling) when prices are high. For the purpose of arbitrage, an ESS owner forecasts the hourly price $\tilde{\lambda}_e$ based on the chosen charge/discharge strategy.

$$R_A = \sum_{t \in T_h} \Big(\tilde{\lambda}_e(t_h)(p_d(t) - p_c(t)) \Big) \tag{6}$$

Reserves/Regulation Provision. ESS can respond to regulation up or regulation down signals in real-time, and therefore can help balance system generation and load. However, ESS needs to plan for reserving part of its capacity to provide such a service. This can be done by optimizing for the ESS capacity to be reserved for future hours, given the forecast of hourly balancing price $\tilde{\lambda}_r$ and error penalty minimization, represented by a penalty factor λ_{mis} multiplied by the difference between the forecast regulation power request signal $\tilde{p}_r(t_r)$ and a battery response $p_b(t_r) = p_d(t_r) - p_c(t_r)$. The regulation signals are sampled at a faster time scale (2-4 seconds), which is represented by $t_r \in \mathbb{T}_r$, where $\mathbb{T}_r$ is the time set of the forecast horizon of the regulation signal.

$$\begin{aligned} R_R = & \sum_{t \in T_h} \Big(\tilde{\lambda}_r(t)\big(p_+(t) + p_-(t)\big) \Big) \\ & - \lambda_{mis} \sum_{t_r \in T_r} |p_b(t_r) - \tilde{p}_r(t_r)|. \end{aligned} \tag{7}$$

Demand Charge Reduction. The ESS can be utilized to reduce the monthly demand charge λ_{pk}, which is estimated using the maximum demand that occurs in a month. The detailed method of calculating demand charge will vary from one utility to another. In this paper, it is assumed that the peak value recorded in the 15-minute interval of the load (in kW) for each month is considered to be charged for peak demand,

$$C_D = \lambda_{pk}\Big(\max_{t_d \in T_d}\big(p_g(t_d)\big)\Big) \tag{8}$$

where $t_d \in \mathbb{T}_d$, is the resolution (usually 15 minutes) for the demand charge calculation and $\mathbb{T}_d$ is the time set of the forecast horizon of the facility load profile.

Power Factor Correction. The power factor shows the utilization of total energy transmitted to loads, i.e., a lower power factor indicates a higher total power needs to be transmitted in order to supply a given load, which in the case of a higher power factor would be satisfied through less power transmission. From (2), the inverter technology can be utilized to maintain reactive power and thus the power factor at the point of common coupling. The cost of the power factor seen by the grid can be calculated through the power factor penalty λ_ρ, which is imposed by the utility as:

$$C_{PF} = \lambda_\rho \max_{t_d \in T_d}\big(0, \rho(t_d) - \rho_+\big), \tag{9}$$

where $\rho(t_d)$ is the power factor at time step t_d:

$$\rho(t_d) = \frac{p_g(t_d)}{|p_g(t_d) + iq_g(t_d)|}, \tag{10}$$

and ρ_+ is the power factor limit imposed by the utility. From above, one may notice how charge/discharge power from the battery, power drawn from the grid, and the power demand at the load are recorded changes from one service to another. At each hourly time-step, the average power drawn to/from the grid and the battery charge/discharge power can be calculated as:

$$p_d(t) = \frac{t_r}{T_h} \sum_{t_r=1}^{t_r \in \mathbb{T}_h} p_d(t_r) + \frac{t_d}{T_h} \sum_{t_d=1}^{t_d \in \mathbb{T}_h} p_d(t_d) + p_d(t_h), \tag{11a}$$

$$p_c(t) = \frac{t_r}{T_h} \sum_{t_r=1}^{t_r \in \mathbb{T}_h} p_c(t_r) + \frac{t_d}{T_h} \sum_{t_d=1}^{t_d \in \mathbb{T}_h} p_c(t_d) + p_c(t_h), \tag{11b}$$

$$p_g(t) = \frac{t_d}{T_h} \sum_{t_d=1}^{t_d \in \mathbb{T}_h} p_g(t_d), \tag{11c}$$

$$\rho(t) = \frac{t_d}{T_h} \sum_{t_d=1}^{t_d \in \mathbb{T}_h} \rho(t_d). \tag{11d}$$

With the above substitution, the system setup shown in (1) – (4) becomes a viable way to track the inter-temporal energy evolution of the ESS and its impact on the grid and load variables.

3. Proposed Methodology

The proposed method follows a sequential approach. First, at each hourly time step, a look-ahead plan (e.g., day-ahead) is constructed, i.e., BESS charge/discharge levels are obtained for the look-ahead horizon (e.g., 24 hours for 1 day). This schedule is then updated every hour based on the most updated real-time information, which is revealed at each hour mark. This section explains these procedures in detail.

3.1. Look-Ahead Plan Formulation

Co-optimization of the above-presented services in the previous section in their most detailed form can be represented as:

$$\begin{aligned}
&\underset{\substack{p_g, p_+, \\ p_-, p_g}}{\text{maximize}} \quad && R_A + R_R - C_D - C_{PF} && \text{(12a)}\\
&\text{subject to} && 0 \le p_d(t) \le p_{max} && \text{(12b)}\\
& && 0 \le p_c(t) \le p_{max} && \text{(12c)}\\
& && x_{min} \le x(t) \le x_{max} && \text{(12d)}\\
& && -(\rho_+) \ge p_g(t)/s_g(t) \ge \rho_+ && \text{(12e)}\\
& && (1) - (5), (11), \forall t \in \mathbb{T}_h, \forall t_r \in \mathbb{T}_r, \forall t_d \in \mathbb{T}_d &&
\end{aligned}$$

The above optimization problem maximizes the revenue (minimizes the cost) from procuring the services subject to internal (battery) and external (service) constraints. The variables in the objectives and constraints are explained in detail in Section 2. Next, we show how the problem (12) in its most comprehensive form is challenging to solve.

3.1.1. Multiple Temporal Dimension

Multi-time-steps involved with multiple services increase the size and thus the computation requirements. For example, the regulation service is performed for every $2-4$ seconds. This makes each variable in the daily look-ahead optimization problem have a large dimension of $21,600$ time steps, considering a regulation signal of 4 seconds. Along with the inter-temporal SoC constraints, these time steps become coupled, making it a very large problem to solve. Moreover, some services have a higher look-ahead duration compared to others. For example, demand charge is determined on a monthly basis, whereas the energy arbitrage is performed on a daily basis.

To mitigate this, service with the longest hour is chosen as the base time-step. For the case of this paper, we use the energy arbitrage service that is performed on an hourly basis. Also, the look-ahead period is adjusted to only cover look-ahead a day in advance. With these changes, the other services (reserves/regulation participation and demand charge reduction) are adjusted accordingly.

The reserves/regulation provision is first split into an hourly calculation of capacity to be reserved and then is adjusted in the real-time reserve market. The BESS then receives a regulation signal that is scaled with its contracted capacity in the subsequent real-time scenario. In the day-ahead reserve market, the benefit of procuring reserves is then represented by (7) without the second term. To assure that enough energy is available in BESS to account for contracted power, the following constraints are implemented:

$$p_-(t) \leq p_{max} - \big(p_c(t) - p_d(t)\big) \tag{13a}$$

$$p_+(t) \leq \big(p_c(t) - p_d(t)\big) + p_{max} \tag{13b}$$

$$0 \leq x(t) - (\eta_d/\eta_c)p_-(t) \leq x_{max}(t) \tag{13c}$$

$$0 \leq x(t) + \eta_c\eta_d p_+(t) \leq x_{max}(t) \tag{13d}$$

Similarly, simplification is done for the demand charge as follows. The demand charge reduction is simplified to be representable with hourly resolution load values and a horizon of 1 day. However, once the peak load to be imported from the grid is calculated for a day, it is maintained in real-time with the actual load measurement. In this way, the peak load is updated for each day and compared with all the days of the month, and eventually the highest peak load for the month is subjected to demand charge. With these assumptions, (11c) is redundant because $p_g(t)$ is assumed to be averaged over demand charge intervals.

3.1.2. Non-Convex Constraints

The constraints (12e), such as power factor correction, introduce non-convexity in the optimization problem. This is difficult to solve with commonly available, efficient off-the-shelf solvers, increases the solution time significantly, and could generate multiple solutions.

The complex apparent power equations related to inverter/grid constraints (2)/(5) can be linearized using a polyhedral norms – first proposed in [38] and then utilized for volt/var control problem in [39]. For the case of this paper, these equivalent linear approximations for inverter apparent power $s_b(t) = |p_b(t) + iq_b(t)| \leq s_{max}$ are:

$$\begin{aligned} -s_{max} \leq p_b(t)cos(l\frac{\pi}{k}) + q_b(t)sin(l\frac{\pi}{k}) & \qquad \leq s_{max} \\ \text{for} \qquad l = 1, \ldots, k. & \end{aligned} \tag{14}$$

3.1.3. Min-Max Structure

We utilized the approximations from the previous section to address the final hurdle in efficiently solving the optimization problem—the min-max structure of objective function introduced due to the demand charge reduction and power factor penalty. Along with the assumption on average power over the hourly time-step, for the demand charge calculation we reformulated the problem by introducing an auxiliary variable p_{pk} as:

$$p_g(t) \leq p_{pk}, \tag{15a}$$

$$p_{pk} \geq 0 \tag{15b}$$

which achieves the objective to minimize the term $\lambda_{pk}p_{pk}$. Similarly, the difficult maximization term of (9) is reformulated using the linearization of the complex apparent term shown in (14). The resultant set of linear equations for power factor correction come out as:

$$\theta(t) \geq 0, \tag{16a}$$
$$\theta(t) \geq \lambda_\rho(p_g(t) - s_g(t)\rho_+) \tag{16b}$$
$$\lambda_\rho\big(p_g(t) - (p_g(t)cos(l\frac{\pi}{k}) + q_g(t)sin(l\frac{\pi}{k}))\rho_+\big) \qquad \leq \theta(t) \tag{16c}$$
$$\lambda_\rho\big(p_g(t) - (p_g(t)cos(l\frac{\pi}{k}) + q_g(t)sin(l\frac{\pi}{k}))\rho_+\big) \qquad \geq -\theta(t) \tag{16d}$$
$$\text{for} \qquad l = \{1, \ldots, k\},$$

which achieves the objective for power factor correction by minimizing $\lambda_\rho\theta(t)$.

3.1.4. Uncertainty Inclusion

The look-ahead problem invariably consists of uncertainties in the form of price (energy/regulation) and load (facility/feeder) predictions. Appropriate procedures for mitigating uncertainty must be implemented; otherwise, severe over/under approximation of service revenue in the look-ahead plan will be observed.

As the above-mentioned subsections demonstrate, the proposed planning stage of this paper attempts to include the desired services from the BESS, while either simplifying or recasting them to exclude their non-convexity and multiple time step complexities. We follow the same philosophy while handling uncertainty associated with the planning stage, by deploying a robust optimization framework [31]. The following reasons explain this framework adoption in detail:

1. A robust counterpart keeps the same complexity as the original problem, i.e., a quadratic program stays quadratic, and a linear program stays linear. For the given framework, as we have recast the planning problem as a linear program (see Section 3.1.2 and Section 3.1.3), this will make the robust counterpart also linear. This has a tremendous positive impact on the practical implication of the planning problem, as most of the off-the-shelf solvers can solve linear programs very efficiently. See [40, 41] and [42] as an example of efficient linear programming solving commercial and open-source solvers, respectively.
2. Robust optimization may not need to quantify the distribution of the uncertain parameter, allowing it to be more flexible to be included for a variety of BESS services. This is especially important for future grid

services, where there may not exist enough data to quantify the uncertain parameter associated with their respective services. This is an advantage of robust optimization, as compared to stochastic optimization [43, 44]. The success of stochastic optimization relies on identifying plausible scenarios for describing uncertain parameters [45]. For the proposed framework of this paper, as the number of services increases, scenarios to identify uncertain parameters may become very large, causing computation intractability. Techniques associated with scenario reductions may be adopted, which may get very complex as the coupling of uncertain parameters may not be easily determined, till enough data has been generated from the field/experiments

Note that a robust optimization framework is known to be conservative in its solution. This is because the aim for robust optimization is to provide a feasible solution for any realization of the uncertainty, and an optimal solution for the worst-case realization of the uncertainty. To manage this conservatism, we utilize the concept of uncertainty budget to tune the conservatism of the robust optimization solution, while defining uncertainty using a compact set (e.g., a polytope) [46, 47]. Hence, the proposed robust optimization framework provides a computationally friendly method to include uncertainties, while providing sufficient modeling flexibility.

The uncertainty in the price variable forecast $\tilde{\lambda}_t$ is accounted for by using the classical robust optimization methodology of accounting for uncertainty using uncertainty budget method [31, 46] as: $\Lambda^e = \{\tilde{\lambda}_e(t') \in \mathbb{R}, \tilde{\lambda}_e(t') \in [\lambda_e^-(t'), \lambda_e^+(t')], \sum_{t' \in T}(\lambda_e^+(t') - \lambda_e^-(t')) \leq \Gamma_A\}$, which shows that $\tilde{\lambda}_e(t')$ is in fact a polytope contained in $[\lambda_{t'}^-, \lambda_{t'}^+]$. Furthermore, the uncertainty set also assumes that the forecast price's maximum deviation is only allowed for up to Γ_A time periods. Meaningful to this context, Γ_A then takes on values in the integer interval $[0, 23]$, where 0 means no price deviation and 24 amounts to price deviation for the whole 24 hour time horizon. The dual from the robust optimization used to account for the uncertainty budget comes out as [31]:

$$\begin{aligned} R_A' = &\sum_{t' \in T} \zeta_A(t') + \Gamma_A \beta_A + \lambda_e(1)(p_d(1) - p_c(1)) \\ &+ \Big(\sum_{t' \in T} \lambda_e^-(t')(p_d(t') - p_c(t'))\Big) \qquad (17a) \\ &\zeta_A(t') \geq 0,\ \beta_A \geq 0,\ t' \in \{2, \ldots, T\}, \qquad (17b) \end{aligned}$$

where the price at the current step $\lambda_e(1)$ is known. For reserve price, uncertainty is defined as: $\Lambda^r = \{\tilde{\lambda}_r(t') \in \mathbb{R}, \tilde{\lambda}_r(t') \in [\lambda_r^-(t'), \lambda_r^+(t')], \sum_{t' \in T}(\lambda_r^+(t') -$

$\lambda_r^-(t')) \leq \Gamma_R\}$, which yields its robust variant as (only shown for reserve up variable):

$$R_R^{'} = \sum_{t' \in T} \zeta_R(t') + \Gamma_R\beta_R + \lambda_r(1)(p_+(1)) + \Big(\sum_{t' \in T} \lambda_r^-(t')(p_+(t'))\Big) \tag{18a}$$

$$\zeta_R(t') \geq 0,\ \beta_R \geq 0,\ t' \in \{2, \dots, T\}, \tag{18b}$$

where the price at the current step $\lambda_r(1)$ is known. Similar equations exist for reserve down and are omitted here for brevity. Finally, for the facility demand to be uncertain and similarly defined in an uncertainty set as $\mathcal{P}_L = \{\tilde{p}_l(t) \in \mathbb{R}, \tilde{p}_l(t) \in [\tilde{p}_l^-(t), \tilde{p}_l^+(t)], \sum_{t \in T}(\tilde{p}_l^+(t) - \tilde{p}_l^-(t)) \leq \Gamma_D\}$:

$$C_D^{'} = \sum_{t \in T} \zeta_D(t) + \Gamma_D\beta_D + \lambda_{pk}p_{pk} \tag{19a}$$

$$\zeta_D(t) + \beta_D \geq \big(\tilde{p}_l^+(t) - \tilde{p}_l^-(t)\big) \tag{19b}$$

$$\zeta_D(t) \geq 0,\ \beta_D \geq 0,\ t \in \{1, \dots, T\}. \tag{19c}$$

3.2. Final Model

Finally, the proposed day-ahead model can be written as

$$\underset{\substack{p_g, p_{pk}, p_+, \\ p_-, p_g, \zeta_D, \\ \beta_D, \zeta_R, \beta_R, \\ \zeta_A, \beta_A}}{\text{maximize}} \quad R_A^{'} + R_R^{'} - C_D^{'} - C_{PF} \tag{20a}$$

$$\text{subject to} \quad (1), (3), (4), (12\text{b}) - (12\text{d}), (13) - (19) \tag{20b}$$

3.3. Extension of Service Selection

Note that we presented the above four use cases in the spirit of covering the most diverse types of services in one portfolio. That is, multiple services may be derived from the above-mentioned service with little or no change in the formulation. Therefore, the presented services are comprehensive in this sense.

3.3.1. Service Extension Framework

The general guidance on extending the proposed framework to more services is as follows.

1. Economic objective of the new service is identified in its full form. For example, see the original objective functions of the arbitrage (6) and reserve revenue (7) services.

2. The intended time-step of the new service, its constraints in full form and their impact on ESS constraints are identified. For example, see the non-convex power factor constraints identified for power factor correction in (10), and multiple time steps of different services identified in (11).
3. For the services identified with the linear constraints and objectives, the intended service can directly go into the proposed framework. However, for the services containing non-convex constraints and different time steps than the identified planning horizon's granularity, they would need to be reworked to be adopted in the proposed framework. Such issues can then be mitigated using the methods described in Section 3.1.1-Section 3.1.3, in detail.
4. Uncertain parameters associated with the respective service are identified and then a robust optimization framework can be adapted to include them, without increasing the optimization problem complexity (see Section 3.1.4)

3.3.2. Services Extension Examples

Examples of the direct extensions from the proposed services of this paper are:

Wholesale Market Services Extensions. The reserve/regulation service modeled using (18) and energy arbitrage service modeled using (17) can be directly expanded to represent other types of services of the wholesale market such as 1) capacity bidding in the ancillary service markets, 2) optimizing for primary regulation, and 3) secondary frequency (load frequency) signals.

Behind-The-Meter Services Extensions. The demand charge reduction service procurement shown in (19), is intended as a local (behind-the-meter) service and can be easily extended to demonstrate as a peak shaving and/or demand shaping service. To implement this extension, rules to incorporate specific shaping/shifting requirements from the net load (facility load minus local renewable generation) can be inputted along with the cost parameters in the objective function and local renewable utilization.

Distribution Grid Services Extensions. The linear power factor correction service constraints implemented using (16) utilize the reactive power capability of the inverter to compensate for the poor power factor. There exist grid services of Volt/Var optimization and conservative voltage reduction (CVR) services that also utilize reactive power injection/absorption [48]. Similar to power factor correction, the objective of such services can be included in the objective function of the proposed framework, and their constraints can be modeled either using a linearization approach of this paper (16) or by using a linear sensitivity factor of the grid location [49, 50].

4. Real-Time Control

Algorithm 1 shows the real-time control sequence of the proposed real-time control algorithm. Once updated information is available, the main part of the real-time control sequence will be implementing the real-time correction rules to incorporate the change in real-time conditions.

Algorithm 1: Real-Time Control Sequence

Input : Base set-point $\tilde{p}$ (charge/discharge) for the hour
Output: Modified set point $\tilde{p}$ (charge/discharge) for each real-time step.

while *Simulation runs* **do**
  if *at beginning of the hour* **then**
    update base set points (charge/discharge) for the current hour using the look-ahead plan for the next day;
  else
    for *each service s in total services* N_s **do**
      for the forecast variable $\tilde{u}$ affecting the service, find its updated conditions $\hat{u}$ – either through measurement or an updated forecast;
      create a rule for a particular service m_s that directly links to the changing condition ;
      update the set points using the rule $\Delta p_s = m_s(\hat{u} - \tilde{u})$;
    end for
    calculate real-time set point for BESS:
    $\tilde{p} = \hat{p} + \sum_{s=1}^{N_s} \Delta p_s$;
    Modify set point if the rules violate the maximum power and energy requirement of the BESS ;
  end if
end while

From the chosen services, the following variables external to the BESS are measured in real-time; (1) actual active power demand $\hat{p}_l$, (2) actual reactive power demand $\hat{q}_l$, (3) real-time energy price $\hat{\lambda}_e$, and (4) real-time reserve price $\hat{\lambda}_r$. In addition to these measurements, real-time market variables such as real-time energy price and reserves price must also be forecast for shorter time-steps (5 minutes).

Note that the accuracy of the real-time updates for forecasts affects the real-time control of BESS because they are directly connected to the decisions. Designing a forecaster for both day-ahead and real-time quantities is out of scope for this work, and interested readers are referred to [33] for forecasting technologies deployed related to BESS applications. Algorithm 1 shows the utilization of updated information in the real-time control algorithm. More specifically, the control is organized around the development of rules to modify in real-time the base set point from the day-ahead planning.

4.1. Real-time Rules

We explain the part Algorithm 1 plays in updating the base set point in real-time in this subsection, as it relates to each specific service. From Algorithm 1, it can be seen that the generic real-time update is done through the equation:

$$\tilde{p} = \hat{p} + \Delta p_s \tag{21}$$

where Δp_s is the change in the base set point for each service s - calculated using a sensitivity rule m_s, which relates the change in actual conditions $\hat{u}$ to predicted conditions $\tilde{u}$, which is calculated using rules calculated from sensitivities:

$$\Delta p_s = m_s(\hat{u} - \tilde{u}). \tag{22}$$

The next subsection demonstrates the calculation of these sensitivities m_s for each considered service s, as adopted in Section 2. The variable t' represent all time steps in the look-ahead horizon where the time-step 1, i.e., $x(1)$, represents the value of variable x for the current hour of the real-time instant t.

Demand Charge. At time step t, the real-time rule for modifying the battery set point with respect to demand charge service is calculated as:

$$m_{dc} = \frac{\frac{\max(\tilde{p}_b(t')) - \min(\tilde{p}_b(t'))}{\mathrm{std}(p_b(\tilde{t}'))}}{\frac{\max(\tilde{p}_l(t')) - \min(\tilde{p}_l(t'))}{\mathrm{std}(p_l(\tilde{t}'))}}, \forall t' \in \{1, \dots N\} \tag{23a}$$

$$\Delta p_{dc} = m_{dc}(\hat{p}_l(t) - \tilde{p}_l(1)). \tag{23b}$$

The demand charge rule is implemented through the sensitivity factor m_{dc}, which attempts to capture the influence of the battery set points output $\tilde{p}_b(t')$ from the optimization problem [1], given the predicted demand variation $\tilde{p}_l(t')$. Once the real-time demand is revealed $\hat{p}_l(t)$, the real-time demand charge correction rule is obtained as Δp_{dc}.

Power Factor Correction. At time step t, the real-time rule for modifying the battery set point with respect to power factor correction service is calculated as:

$$m_{pfc} = \frac{\frac{\max(\tilde{q}_b(t'))-\min(\tilde{q}_b(t'))}{\mathrm{std}(\tilde{q}_b(t'))}}{\frac{\max(\tilde{q}_l(t'))-\min(\tilde{q}_l(t'))}{\mathrm{std}(q_l(\tilde{t}'))}}, \forall t' \in \{1, \ldots N\} \tag{24a}$$

$$\Delta q_{pfc} = m_{dc}(\hat{q}_l(t) - \tilde{q}_l(1)). \tag{24b}$$

The power factor correction rule is implemented through the sensitivity factor m_{pfc}, which attempts to capture the influence of battery reactive power set point output $\tilde{q}_b(t')$ from the optimization problem [1], given the predicted reactive power demand variation $\tilde{q}_l(t')$. Once the real-time reactive power demand is revealed $\hat{q}_l(t)$, the real-time power factor correction rule is obtained as Δq_{pfc}, which is the required reactive power set point for the battery. In this way, Δq_{pfc} represents the extra reactive power to be injected/absorbed using the BESS inverter. This local supply of reactive power by the BESS helps to improve the power factor at the PCC, as it counteracts the reactive power imports from the grid.

Energy Arbitrage. At time step t, the real-time rule for modifying the battery set point with respect to a real-time energy market opportunity is calculated as:

$$m_{ea} = \frac{\frac{\max(\tilde{p}_b(t'))-\min(\tilde{p}_b(t'))}{\mathrm{std}(\tilde{p}_b(t'))}}{\frac{\max(\tilde{\lambda}_e(t'))-\min(\tilde{\lambda}_e(t'))}{\mathrm{std}(\tilde{\lambda}_e(t'))}}, \forall t' \in \{1, \ldots N\} \tag{25a}$$

$$\Delta p_{ea} = m_{ea}(\hat{\lambda}_e(t) - \tilde{\lambda}_e(1)). \tag{25b}$$

The real-time energy market arbitrage rule is implemented through the sensitivity factor m_{ea}, which attempts to capture the influence of battery power set point output $\tilde{p}_b(t')$ from the optimization problem [1], given the day-ahead energy price variation $\tilde{\lambda}_e(t')$. Once the real-time energy price is revealed $\hat{\lambda}_e(t)$, the real-time arbitrage rule is obtained as Δp_{ea}.

Reserve/Regulation Placement. At time step t, the real-time rule for modifying the battery set point with respect to a real-time reserve market opportunity is calculated as:

$$m_{res} = \frac{\frac{\max(\tilde{p}_b(t'))-\min(\tilde{p}_b(t'))}{\mathrm{std}(\tilde{p}_b(t'))}}{\frac{\max(\tilde{\lambda}_r(t'))-\min(\tilde{\lambda}_r(t'))}{\mathrm{std}(\tilde{\lambda}_r(t'))}}, \forall t' \in \{1, \ldots N\} \tag{26a}$$

$$\Delta p_{res} = m_{res}(\hat{\lambda}_r(t) - \tilde{\lambda}_r(1)). \tag{26b}$$

The real-time energy market arbitrage rule is implemented through the sensitivity factor m_{res}, which attempts to capture the influence of the battery power set point output $\tilde{p}_b(t')$ from the optimization problem [1], given the day-ahead reserve price variation $\tilde{\lambda}_r(t')$. Once the real-time reserve price is revealed $\hat{\lambda}_e(t)$, the real-time reserve market rule is obtained as Δp_{res}. The regulation signal is scaled by this capacity Δp_{res}, and the BESS is made to follow it for each real-time step.

Finally, these rules are aggregated to obtain the final real-time battery set point for both active and reactive power as:

$$\hat{p}_b(t) = \tilde{p}_b(t) + \Delta p_{dc} + \Delta p_{ea} + \Delta p_{res} \tag{27a}$$

$$\hat{q}_b(t) = \tilde{q}_b(t) + \Delta q_{pfc} \tag{27b}$$

4.2. Real-Time Control Implementation

Algorithm 1 contains simple rules to adjust the base set-point from the planning optimization, and hence continues to run for each real-time step till the end of the simulation. This means that the real-time control is meant to be operable with an actual BESS, where the setpoints are autonomously changed throughout its operation in the direction of improving the BESS revenue, as depicted in rules (23) – (26). Because real-time control is implemented through rules, it may not end up violating physical and market constraints, which need to be manually implemented. First, the real-time set points generated by (27) must be verified against the BESS's energy, power, and inverter capacity limitations. In case of violation, they are manually adjusted using system power balance equations (1)-(4). Second, for an efficient real-time energy market, participants must oblige to their bid/cleared quantities. To this end, we limit the charge/discharge quantity of BESS, based on whether it will violate the real-time energy market commitment. For example, if a BESS commits to dispatch at 5 kW of discharge power (selling energy), then the algorithm sets this as a threshold for discharge power commitment. That is, if the real-time rules for services other than arbitrage cause the BESS to violate this threshold of the discharge power, then those service violations will be limited using such thresholds. Finally, the real-time control (actual seconds-to-seconds implementation) violations due to uncertainties are penalized to demonstrate the realistic operation of increase in cost due to non-compliance of market service. For example, for regulation service, we implement a penalty factor, which penalizes BESS if it does not follow the regulation signal. That is, we use (7) to calculate the actual revenue, where λ_{miss} is set as 0.8 [51]. This means that for every MW deviation from the instructed regulation dispatch, 80% reduction in revenue is assumed [52], which is a simplification of ISOs' ancillary services performance model, as pointed out in [53]. The demand charge reduction and power factor corrections do not really have any consequences of not meeting the contracted values and are therefore not implemented as binding services.

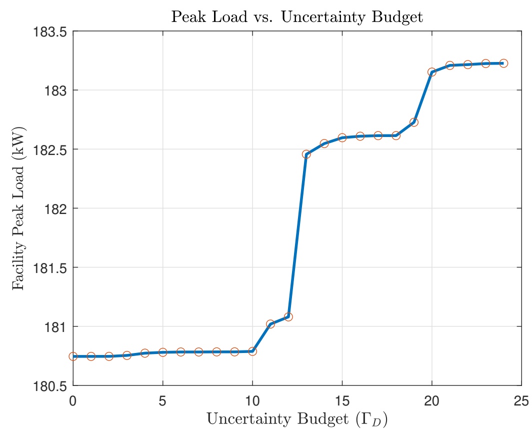

Figure 2: Impact on individual service optimization with an increase in the uncertainty budget—demonstration of peak load minimization.

4.3. Real-Time Modeling Extension

From Algorithm 1 and (23)-(27), it can be seen that the real-time adjustment algorithm consists of simple rules and thus can incorporate higher-fidelity SoC modeling of the BESS, such as in [54]. Even though this is out of scope for this work, this feature may be desirable for studies evaluating operation losses of BESS to incorporate multiple services. A suitable approach for including such SoC models is as follows. The look-ahead plan can include the approximation BESS model, while the real-time control can then include a higher-fidelity model [54] of the same approximation deployed in the look-ahead stage.

5. Simulation Results

The proposed setup is tested with a utility-scaled BESS that has an energy/power capacity of 1,500 kWh/750 kW. The power factor limit of 0.95 at PCC is used—to support that, a 1,000 kVA inverter rating is assumed. This gives the BESS the ability to provide 665 kVar at the rated power. The load data from one of the large commercial buildings in the north pacific region of the USA is used. To generate energy and reserve prices for both day-ahead and real-time markets, historical data from a real ISO is used [55]. The look-ahead optimization time horizon is chosen as 24 hours with 1-hour resolution, whereas the real-time market signals are updated every 5 minute, and then eventually the real-time control is implemented every second. We use zero mean with fixed variance random variables to generate day-ahead and real-time market variable forecasts. However, to run the parametric simulations, the seed functionality for Python is used to duplicate the random variables for fair comparison. Similarly, the historical regulation

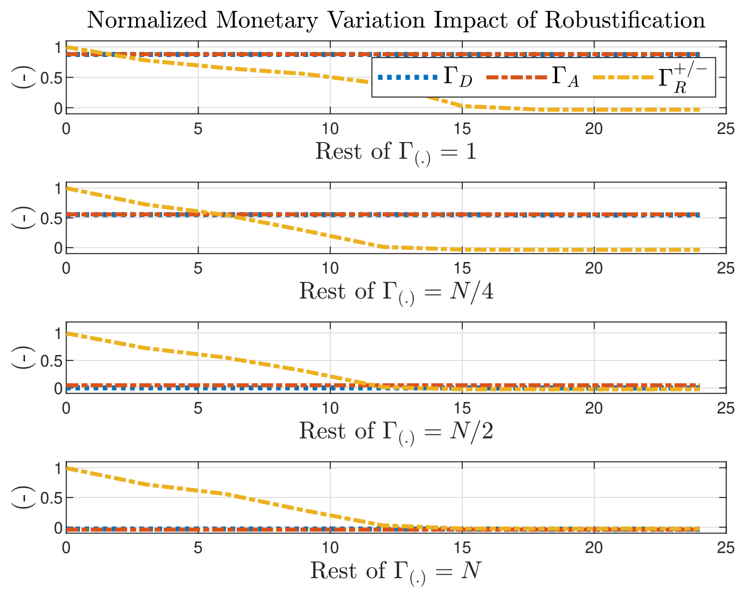

Figure 3: Impact on revenue normalized to maximum value (y-axis) as the budget uncertainty $\Gamma_{(.)}$ (x-axis) changes.

signal from [55] is used as the actual regulation instruction so that fair comparison between real-time adjustments is obtained. To simulate a realistic utility operation where the BESS helps provide power during outages, we keep 20% of the energy as the reserve for the possibility of the outage event. The planning problem's optimization problem is implemented using PYOMO [56] with GLPK as an open-source solver [42].

5.1. Tuning Robust Optimization Based Planning Problem

Before the look-ahead model is set up, budget uncertainty parameters need to be tuned. This is done to select uncertainty budget parameters such that they provide a right balance between the conservatism of the solution and handling uncertainty. Figure 2 shows the impact of increasing the budget of uncertainty on the selected peak load threshold picked by the optimization problem. As expected, with a higher value of the demand charge uncertainty budget, the optimization picks a more conservative solution, accounting for higher peak load optimization for the day-ahead period. For a fair comparison, the results of Fig. 2 are produced with the fixed load forecast values.

Figure 3 presents the influence on the individual service revenue/cost because its uncertainty budget is varied from 0 to N (N=24 hours), while keeping the other services in the co-optimization at a fixed uncertainty budget at: (1) 1 (top most subplot), (2) N/4 (top middle), (3) N/2 (bottom middle), and (4) N (bottom most plot). From Fig. 3, demand charge and energy arbitrage services are influenced by the uncertainty budget of not only their own services, but also of the other services. This is because the term related to reserve/regulation energy dominates the objective function. This can also be seen for the revenue degradation of reserve/regulation services as its uncertainty budget increases. To strike a balance for mitigating future uncertainties and assuring revenue in the day-ahead market, we select a budget uncertainty of (N/4) 6 hours.

5.2. Quantitative Results Comparison

Figure 4 shows the results from a 1-month run with both the predicted day-ahead (DA) values and their actual realized real-time (RT) values. The BESS' SoC (bottom plot) stays within the reserve SoC for the entire duration while the BESS supports the grid by minimizing the peak load (middle plot). In the middle plot, the "total load" is the facility load target of which a portion is contributed by the BESS discharging (top plot). Notice that around times "2019-01-13 – 2019-01-17" the real-time load became higher than the predicted peak load; however, it was decreased by the BESS discharging and thus supporting the local load. Moreover, due to allowing for a higher load (robust optimization) in the look-ahead optimization and utilizing the real-time conditions to adjust set points in real-time, the actual peak load is less than the predicted DA peak load. One day from the month-long run is presented in Fig. 5, with the reference peak load for that day. Notice that the BESS flattens the grid load imported to the facility. It also places commitments for other services (arbitrage/reserves) in the DA market and then provides corrections based on real-time measurements (load/actual regulation signal) and market (energy/reserve) signals. Also, the day-ahead predicted peak load is higher due to robust optimization incorporation. The reactive power supplied by the BESS and the resulting power factor at the PCC for the month-long run is shown in Fig. 6. During times of high mismatch between the predicted and the actual facility load, the reactive power drops (e.g., around 2019-01-17). This is because of the higher need for active power to assure that financial revenue during these times reduces the available reactive power capacity. However, throughout the simulation, it stays within the prescribed limit of 0.95. The overall revenue obtained from the BESS operation of Fig. 4 and Fig. 6 is shown in Table 2 where the importance of including real-time (RT) adjustment is shown as an improvement of 3.7% from the DA economic estimation. Almost all individual service revenue (negative cost) improves. The primary savings comes from reserve/regulation service. Also, note that this improvement is due to real-time adjustment (3.7%) and should be seen as an addition to the already estimated positive revenue expected in the day-ahead look-ahead planning stage. Now, the real-time adjustment not

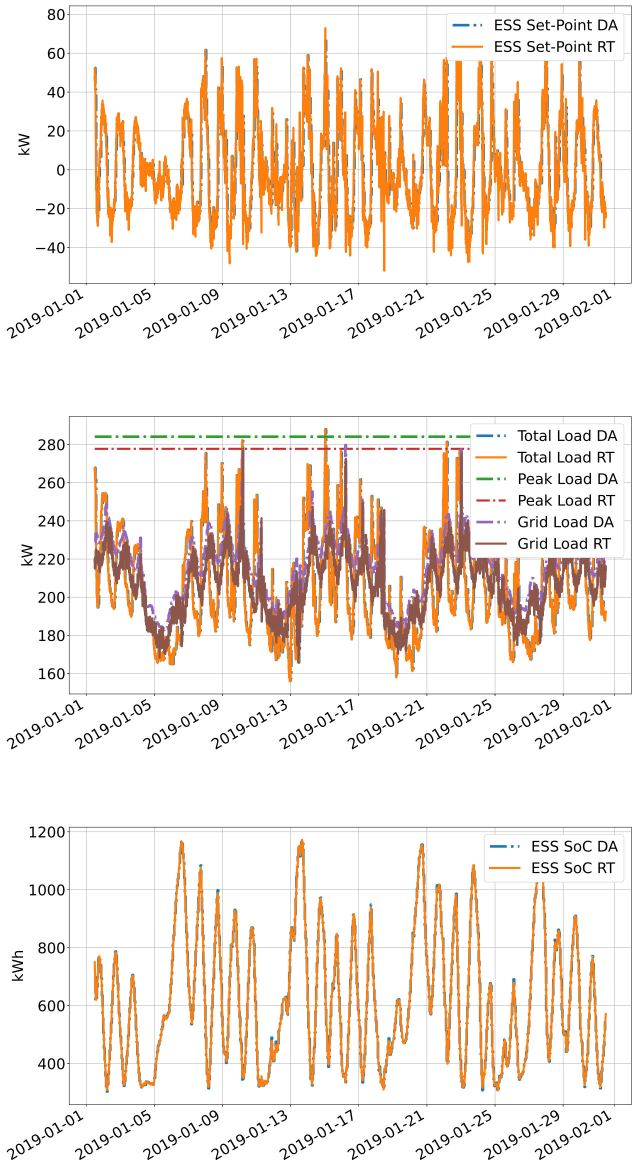

Figure 4: Battery set points (top), resulting grid power flows load import (middle), and resulting BESS SoC (bottom).

only attempts to maintain this increase, but also improves upon it.

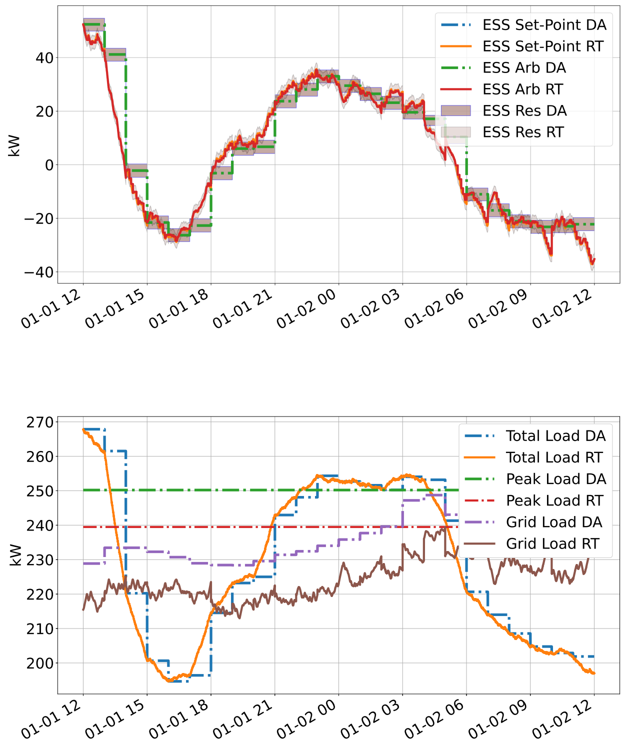

Figure 5: Battery set point with individual services set points, the individual services set point (top), and the net grid load import and peak load (bottom)

Table 2: One-month revenue for different services with planned (DA) and its improvement through real-time (RT) correction.

Service	DA ($)	RT ($)	Improved (%)
Demand Charge	303.04	301.81	0.40
Reserve/Regulation	1175.53	1203.30	2.36
Energy Arbitrage	23.89	28.22	18.1
Total	896.38	929.71	3.71

5.3. Implementation Remarks

Finally, we present remarks on the scalable, modular, and computationally efficient nature of the proposed method. Table 2 lists the solution time taken by

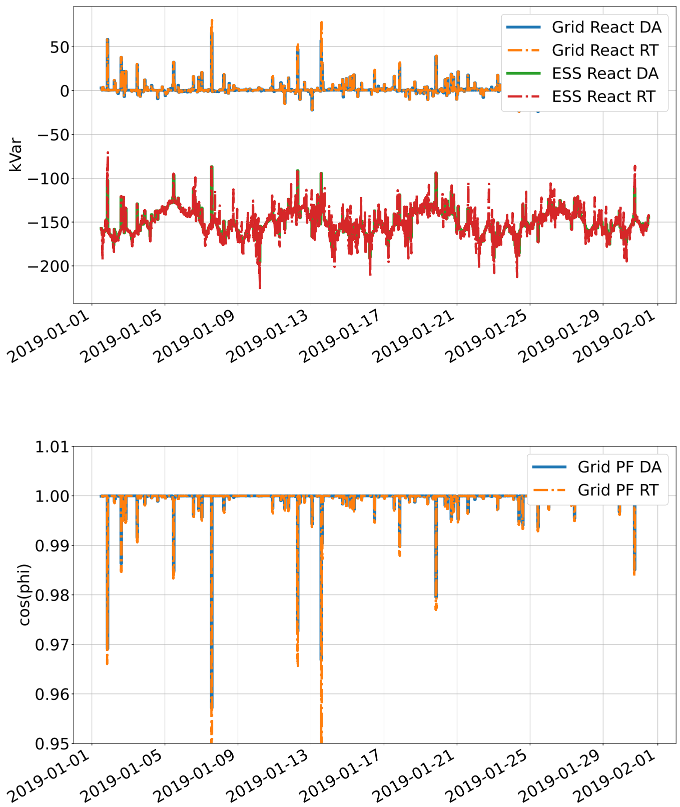

Figure 6: Reactive power dispatch (top) and the resultant power factor measured at PCC (bottom)

the implemented program to include service in the proposed framework. That is, the time it takes to perform a day-ahead planning stage and the real-time control for the particular service. It can be seen from Table 2, that the planning problem of the proposed framework, scales well, as more and more services are included. Even with all services included, the planning problem takes approximately 1 second to complete. The largest increase in the planning problem solution time is seen by the addition of power factor correction constraints, as it has the highest number of service-specific constraints (16). For power system services scheduling (e.g. day-ahead energy procurement), resolution of hourly or half/hourly is sufficient. Hence, the proposed framework can easily be included in such a time frame to support BESS services procurement.

For the RT control implementation, since they are calculated using a sensitivity factor, which is calculated at the top of the hour, the increase in solution time due to increase in number of control laws is almost negligible. One of the fastest known BESS services can be the primary frequency regulation, which is performed on a 2-4 seconds basis. Even for such fast service delivery requirement, the proposed real-time control framework can be easily integrated with real-time service requests of power grid. In Table 3, a slight increase in the real-time control implementation can be noticed when power factor correction rules are included. This may be due to the extra conditions related to inverter sizes and available reactive power supply.

The results presented in Table 3, were verified for multiple simulation instantiating. For the same uncertain parameter sets, the initial conditions and random variable generation (using Python's seed functionality), the same results were obtained for all instances. This is because 1) the final optimization problem is a linear program, which has a global minimum, and 2) the control laws follow the planning stage's result, similar real-time sensitivity factors were obtained.

Table 3: Solution time with addition of services using the proposed Framework. The notation used in the table are as follows: Demand Charge (DC), Energy Arbitrage (EA), Reserve/Regulation (RR), Power Factor Correction (PFC).

Service	DA Time (sec.)	RT Time (sec.)
DC	0.32	3.1e-3
DC + RR	0.61	3.1e-3
DC + RR + EA	0.72	3.1e-3
DC + RR + EA + PFC	1.08	3.2e-3

6. Conclusion & Future Works

In this paper, we presented the multi-service procurement framework of the BESS. The novelty of the proposed framework was that it was able to handle complications arising from multiple time scales of planning and operation phases, as well as service dependent requirements. This was achieved using linearization and robustification techniques which mitigated non-convexities and uncertainties in the formulation so that all services can be cast in a unified framework. In doing so, it was also shown that the proposed framework can be extended to many more services and BESS operation techniques. Simulations were carried out to demonstrate the efficacy of the proposed framework. It was shown the method takes advantage of a two-step (planning and operation) procedure to improve the BESS revenue. Moreover, it was demonstrated that the proposed method scales well, i.e., it appropriately handles the computational burden of including multiple services. Hence, the proposed method can be integrated into the current power systems planning and operation phases.

Since the focus of this work was towards multiple service procurement through the planning and control of BESS, the presented work assumed a relatively simple model for 1) the BESS ownership, 2) the electric grid connections, and 3) the battery chemistry. Hence, we recognize a few interesting future works to further improve the proposed multi-service procurement framework. First, multiple ownership models of the BESS (e.g., residential owner versus an aggregator) may be explored. The choices of privacy considerations, market rules/regulatory barriers in the ownership models, and its implications for the proposed multi-service framework may be explored. Second, the placement of BESS in the various portion of the grid (transmission or distribution) impacts the relevant electric grid constraints in the multi-service framework. Future work may explore such constraints. Finally, the last recognized future work is the exploration of suitable battery chemistry models to be represented in planning and real-time control of the proposed framework. As both planning and real-time control have different time granularity, the models may need to be adjusted to achieve a trade-off between accuracy and computational efficiency.

References

[1] J. Alam, P. Balducci, K. Whitener, S. Cox, Energy storage control capability expansion: Achieving better technoeconomic benefits at portland general electric's salem smart power center, IEEE Power and Energy Magazine 18 (2) (2020) 69–80. doi:10.1109/MPE.2019.2959115.

[2] M. H. Mostafa, S. H. Abdel Aleem, S. G. Ali, Z. M. Ali, A. Y. Abdelaziz, Techno-economic assessment of energy storage systems using annualized life cycle cost of storage (lccos) and levelized cost of energy (lcoe) metrics, Journal of Energy Storage 29 (2020) 101345. doi:https://doi.org/10.1016/j.est.2020.101345.
URL `http://www.sciencedirect.com/science/article/pii/S2352152X19316925`

[3] M. K. Metwaly, J. Teh, Probabilistic peak demand matching by battery energy storage alongside dynamic thermal ratings and demand response for enhanced network reliability, IEEE Access 8 (2020) 181547–181559.

[4] M. K. Metwaly, J. Teh, Optimum network ageing and battery sizing for improved wind penetration and reliability, IEEE Access 8 (2020) 118603–118611.

[5] J. Teh, C.-M. Lai, Reliability impacts of the dynamic thermal rating and battery energy storage systems on wind-integrated power networks, Sustainable Energy, Grids and Networks 20 (2019) 100268.

[6] P. Balducci, K. Mongird, M. J. Alam, D. Wu, V. Fotedar, V. Viswanathan, A. Crawford, Y. Yuan, G. Labove, S. Richards, X. Shane, K. Wallace, Washington clean energy fund grid modernization projects: Economic analysis, Tech. rep., Pacific Northwest National Lab.(PNNL), Richland, WA (United States) (2020).

[7] K. Mongird, V. V. Viswanathan, P. J. Balducci, M. J. E. Alam, V. Fotedar, V. S. Koritarov, B. Hadjerioua, Energy storage technology and cost characterization report, Tech. rep., Pacific Northwest National Lab.(PNNL), Richland, WA (United States) (2019).

[8] P. Balducci, M. J. Alam, T. McDermott, V. Fotedar, X. Ma, D. Wu, B. A. Bhatti, K. Mongird, B. Bhattarai, A. Crawford, S. Ganguli, Nantucket island energy storage system assessment, Tech. rep., Pacific Northwest National Lab.(PNNL), Richland, WA (United States) (2019).

[9] P. J. Balducci, M. J. E. Alam, T. D. Hardy, D. Wu, Assigning value to energy storage systems at multiple points in an electrical grid, Energy Environ. Sci. 11 (2018) 1926–1944. doi:10.1039/C8EE00569A.
URL `http://dx.doi.org/10.1039/C8EE00569A`

[10] M. J. E. Alam, P. J. Balducci, T. D. Hardy, A. Bose, C.-C. Liu, A. K. Srivastava, Y. Xu, T. J. Morrell, V. Venkatramanan, Y. Zhang, C. Liu, Development and analysis of control strategies for a 1 mw/3.2 mwh energy storage system at avista utilitiesdoi:10.2172/1647922.
URL `https://www.osti.gov/biblio/1647922`

[11] P. Heine, H. Hellman, A. Pihkala, K. Siilin, Battery energy storage for distribution system – case helsinki, in: 2019 Electric Power Quality and Supply Reliability Conference (PQ) 2019 Symposium on Electrical Engineering and Mechatronics (SEEM), 2019, pp. 1–6. doi:10.1109/PQ.2019.8818258.

[12] ComEd Conducting Illinois' First Community Energy Storage Pilot, `https://www.comed.com/News/Pages/NewsReleases/2017`$_03_16.aspx, accessed : 2020-12-01$.

[13] R. Kini, D. Raker, T. Stuart, R. Ellingson, M. Heben, R. Khanna, Mitigation of pv variability using adaptive moving average control,

IEEE Transactions on Sustainable Energy 11 (4) (2020) 2252–2262. doi:10.1109/TSTE.2019.2953643.

[14] J. Marchgraber, W. Gawlik, Dynamic prioritization of functions during real-time multi-use operation of battery energy storage systems, Energies 14 (3) (2021). doi:10.3390/en14030655.
URL https://www.mdpi.com/1996-1073/14/3/655

[15] M. Ghazavidozein, O. Gomis-Bellmunt, P. Mancarella, Simultaneous provision of dynamic active and reactive power response from utility-scale battery energy storage systems in weak grids, IEEE Transactions on Power Systems (2021) 1–1doi:10.1109/TPWRS.2021.3076218.

[16] S. Hanif, B. B. P. B. Alam, M. J. E., T. E. McDermott, A modular optimal power flow method for integrating new technologies in distribution grids, in: 2020 IEEE Power Energy Society General Meeting (PESGM), 2020, pp. 1–5. doi:10.1109/PESGM41954.2020.9281907.

[17] B. A. Bhatti, S. Hanif, M. J. E. Alam, T. E. McDermott, P. Balducci, A combined day-ahead and real-time scheduling approach for real and reactive power dispatch of battery energy storage, in: 2020 IEEE Power Energy Society General Meeting (PESGM), 2020, pp. 1–5. doi:10.1109/PESGM41954.2020.9281982.

[18] E. Namor, F. Sossan, R. Cherkaoui, M. Paolone, Control of battery storage systems for the simultaneous provision of multiple services, IEEE Transactions on Smart Grid 10 (3) (2019) 2799–2808. doi:10.1109/TSG.2018.2810781.

[19] M. U. Hashmi, D. Deka, A. Bušić, L. Pereira, S. Backhaus, Arbitrage with power factor correction using energy storage, IEEE Transactions on Power Systems 35 (4) (2020) 2693–2703. doi:10.1109/TPWRS.2020.2969978.

[20] H. J. Kim, R. Sioshansi, A. J. Conejo, Benefits of stochastic optimization for scheduling energy storage in wholesale electricity markets, Journal of Modern Power Systems and Clean Energy (2020) 1–9doi:10.35833/MPCE.2019.000238.

[21] A. Schroeder, Modeling storage and demand management in power distribution grids, Applied Energy 88 (12) (2011) 4700 – 4712. doi:https://doi.org/10.1016/j.apenergy.2011.06.008.
URL http://www.sciencedirect.com/science/article/pii/S0306261911003783

[22] Stochastic optimal sizing of distributed energy resources for a cost-effective and resilient microgrid, Energy 198 (2020) 117284. doi:https://doi.org/10.1016/j.energy.2020.117284.

[23] T. Qiu, B. Xu, Y. Wang, Y. Dvorkin, D. S. Kirschen, Stochastic multistage coplanning of transmission expansion and energy storage, IEEE Transactions on Power Systems 32 (1) (2017) 643–651. doi:10.1109/TPWRS.2016.2553678.

[24] Y. Shi, B. Xu, D. Wang, B. Zhang, Using battery storage for peak shaving and frequency regulation: Joint optimization for superlinear gains, IEEE Transactions on Power Systems 33 (3) (2018) 2882–2894. doi:10.1109/TPWRS.2017.2749512.

[25] H. Yuan, F. Li, Y. Wei, J. Zhu, Novel linearized power flow and linearized opf models for active distribution networks with application in distribution lmp, IEEE Transactions on Smart Grid (2016) 1doi:10.1109/TSG.2016.2594814.

[26] J. Kim, Y. Choi, S. Ryu, H. Kim, Robust operation of energy storage system with uncertain load profiles, Energies 10 (4) (2017) 416.

[27] A. A. Thatte, L. Xie, D. E. Viassolo, S. Singh, Risk measure based robust bidding strategy for arbitrage using a wind farm and energy storage, IEEE Transactions on Smart Grid 4 (4) (2013) 2191–2199. doi:10.1109/TSG.2013.2271283.

[28] R. A. Jabr, I. Džafić, B. C. Pal, Robust optimization of storage investment on transmission networks, IEEE Transactions on Power Systems 30 (1) (2015) 531–539. doi:10.1109/TPWRS.2014.2326557.

[29] R. A. Jabr, A primal-dual interior-point method to solve the optimal power flow dispatching problem, Optimization and Engineering 4 (4) (2003) 309–336. doi:10.1023/B:OPTE.0000005390.63406.1e.
URL `https://doi.org/10.1023/B:OPTE.0000005390.63406.1e`

[30] H. Almasalma, G. Deconinck, Simultaneous provision of voltage and frequency control by pv-battery systems, IEEE Access 8 (2020) 152820–152836. doi:10.1109/ACCESS.2020.3018086.

[31] A. Ben-Tal, A. Nemirovski, Robust convex optimization, Mathematics of Operations Research 23 (4) (1998) 769–805. doi:10.1287/moor.23.4.769.

[32] D. L. Rodrigues, X. Ye, X. Xia, B. Zhu, Battery energy storage sizing optimisation for different ownership structures in a peer-to-peer energy sharing community, Applied Energy 262 (2020) 114498. doi:https://doi.org/10.1016/j.apenergy.2020.114498.
URL `https://www.sciencedirect.com/science/article/pii/S0306261920300106`

[33] R. H. Byrne, T. A. Nguyen, D. A. Copp, B. R. Chalamala, I. Gyuk, Energy management and optimization methods for grid energy storage systems, IEEE Access 6 (2018) 13231–13260. doi:10.1109/ACCESS.2017.2741578.

[34] Asian Development Bank, Handbook on Battery Energy Storage System, Asian Development Bank, Metro Manila, Philippines, 2018. doi:http://dx.doi.org/10.22617/TCS189791-2.

[35] Market Rule 1: Standard Market Design, https://www.iso-ne.com/participate/rules-procedures/tariff/market-rule-1, accessed August 2020.

[36] E. D. Cartwright, Ferc order 2222 gives boost to ders (2020).

[37] J. McLaren, P. Gagnon, K. Anderson, E. Elgqvist, R. Fu, T. Remo, Battery energy storage market: Commercial scale, lithium-ion projects in the u.s.
URL `https://www.osti.gov/biblio/1337480`

[38] A. Ben-Tal, A. Nemirovski, Lectures on modern convex optimization: analysis, algorithms, and engineering applications, SIAM, 2001.

[39] R. A. Jabr, Linear decision rules for control of reactive power by distributed photovoltaic generators, IEEE Transactions on Power Systems 33 (2) (2018) 2165–2174. doi:10.1109/TPWRS.2017.2734694.

[40] Gurobi Optimization, Gurobi optimization (2016).
URL `http://www.gurobi.com`

[41] IBM, IBM ILOG CPLEX Optimization Studio (2015).
URL `http://www-03.ibm.com/software/products/en/ibmilogcpleoptistud`

[42] GLPK, GLPK: GNU linear programming toolkit (2009).
URL `http://www.gnu.org/software/glpk/`

[43] W. B. Powell, S. Meisel, Tutorial on stochastic optimization in energy—part i: Modeling and policies, IEEE Transactions on Power Systems 31 (2) (2016) 1459–1467. doi:10.1109/TPWRS.2015.2424974.

[44] W. B. Powell, S. Meisel, Tutorial on stochastic optimization in energy—part ii: An energy storage illustration, IEEE Transactions on Power Systems 31 (2) (2016) 1468–1475. doi:10.1109/TPWRS.2015.2424980.

[45] A. J. Conejo, M. Carrión, J. M. Morales, et al., Decision making under uncertainty in electricity markets, Vol. 1, Springer, 2010.

[46] J. M. Morales, A. J. Conejo, H. Madsen, P. Pinson, M. Zugno, Integrating Renewables in Electricity Markets, Vol. 205 of International Series in Operations Research & Management Science, Springer US, Boston, MA, 2014. doi:10.1007/978-1-4614-9411-9.

[47] M. Nazari-Heris, B. Mohammadi-Ivatloo, Application of robust optimization method to power system problems, Classical and recent aspects of power system optimization (2018) 19–32.

[48] R. A. Jabr, Robust volt/var control with photovoltaics, IEEE Transactions on Power Systems 34 (3) (2019) 2401–2408. doi:10.1109/TPWRS.2018.2890767.

[49] A. Bernstein, E. Dall'Anese, Linear power-flow models in multiphase distribution networks: Preprint, in: IEEE International Conference on Innovative Smart Grid Technologies (ISGT Europe 2017), 2017.
URL `http://www.osti.gov/scitech/servlets/purl/1361015`

[50] K. Baker, A. Bernstein, E. Dall'Anese, C. Zhao, Network-cognizant voltage droop control for distribution grids, IEEE Transactions on Power Systems 33 (2) (2018) 2098–2108. doi:10.1109/TPWRS.2017.2735379.

[51] Y. Shi, B. Xu, D. Wang, B. Zhang, Using battery storage for peak shaving and frequency regulation: Joint optimization for superlinear gains, IEEE Transactions on Power Systems 33 (3) (2017) 2882–2894.

[52] B. Xu, Y. Dvorkin, D. S. Kirschen, C. A. Silva-Monroy, J.-P. Watson, A comparison of policies on the participation of storage in u.s. frequency regulation markets, in: 2016 IEEE Power and Energy Society General Meeting (PESGM), 2016, pp. 1–5. doi:10.1109/PESGM.2016.7741531.

[53] B. Xu, Batteries in electricity markets: economic planning and operations, Ph.D. thesis (2018).

[54] A. J. Crawford, V. V. Viswanathan, M. J. E. Alam, P. J. Balducci, D. Wu, C. K. Vartanian, K. Mongird, Snohomish public utility district mesa 2: An assessment of flow battery energy storage system technical performance, Tech.

rep., Pacific Northwest National Lab.(PNNL), Richland, WA (United States) (2019).

[55] Pennsylvania, Jersey, Maryland Power Pool (PJM), Regulation market data (2017).
URL https://tinyurl.com/2p83u265

[56] W. E. Hart, J.-P. Watson, D. L. Woodruff, Pyomo: modeling and solving mathematical programs in python, Mathematical Programming Computation 3 (3) (2011) 219–260.

Highlights

- Novel method to explicitly address services pertaining to behind-the-meter, system-wide and reactive power applications, with demonstration of multiple services procurements of i) energy arbitrage, ii) demand charge reduction, iii) reserve/regulation provision and iv) power factor correction.
- The proposed look-ahead optimization handles difficulties such as: i) multiple temporal dimensions, ii) non-convexity constraints, iii) min-max structure and iv) uncertainty related to external variables, arising due to multiple services procurement
- The real-time control using sensitivity-based rules is proposed for timely modification of charge/discharge signal for the BESS.